AIAA 2003-4240

Uncertainty Propagation for Turbulent, Compressible Flow in a Quasi-1D Nozzle Using Stochastic Methods

Lionel Mathelin and M. Yousuff Hussaini
Florida State University
Tallahassee, Florida

Thomas A. Zang
NASA Langley Research Center
Hampton, Virginia

Françoise Bataille
Centre de Thermique de Lyon
Villeurbanne, France

16th AIAA Computational Fluid Dynamics Conference
June 23–26, 2003/Orlando, FL

Uncertainty Propagation for Turbulent, Compressible Flow in a Quasi-1D Nozzle Using Stochastic Methods

Lionel Mathelin,* M. Yousuff Hussaini,† Thomas A. Zang‡ and Françoise Bataille§

This paper describes a fully spectral, Polynomial Chaos method for the propagation of uncertainty in numerical simulations of compressible, turbulent flow, as well as a novel stochastic collocation algorithm for the same application. The stochastic collocation method is key to the efficient use of stochastic methods on problems with complex nonlinearities, such as those associated with the turbulence model equations in compressible flow and for CFD schemes requiring solution of a Riemann problem. Both methods are applied to compressible flow in a quasi-one-dimensional nozzle. The stochastic collocation method is roughly an order of magnitude faster than the fully Galerkin Polynomial Chaos method on the inviscid problem.

Introduction

An admittedly small but nevertheless noticeably accelerating trend within the Computational Fluid Dynamics (CFD) community is changing the vision of computational aerodynamics from one of producing a solution as accurately as possible to one of producing a solution with acceptable uncertainty bounds. Most of the effort of the traditional CFD community has been focused on discretization error and turbulence modeling error. Some of the early advocates of a broader perspective on CFD uncertainty were Mehta,[1] Roache,[2] Coleman and Stern[3] and Oberkampf and Blottner.[4] In the past half-dozen years there have been several events which have served to increase awareness of the broader perspective on CFD uncertainty: (1) the publication of the American Institute for Aeronautics and Astronautics guidelines on the verification and validation for CFD;[5] (2) the Drag Prediction Workshop sponsored by the AIAA Applied Aerodynamics TC;[6] and (3) the pair of sessions on CFD uncertainty at the January, 2003 AIAA Aerospace Sciences Meeting.[7–19] The work of Oberkampf, Deigert, Alvin and Rutherford[20] and Oberkampf and Trucano[21] is especially notable for proposing a framework for characterization of uncertainties. Walters and Huyse[22] have provided a tutorial on uncertainty methods aim at a CFD audience. Hemsch, Luckring and Morrison[10] have presented a comprehensive vision for approaching computational aerodynamics uncertainty. (Their choice of title is noteworthy in that their vision is not confined to Euler and Navier-Stokes methods but embraces the use of simpler aerodynamic models.) Zang, *et al*[23] have outlined the needs and opportunities for uncertainty quantification and optimization under uncertainty research for aerospace applications.

Some, but by no means all of the uncertainties affecting CFD are reasonably described in probabilistic terms. (See Oberkampf, Helton and Sentz[24] for a general mathematical framework for describing uncertainties.) Our focus in this work is on stochastic methods for quantifying those uncertainties which can be described by probability density functions (PDFs). A fundamental task for these methods is to propagate prescribed uncertainty distributions on the input parameters, *e.g.*, boundary conditions, or code parameters, *e.g.*, turbulence modeling coefficients, through the CFD code to the output field variables and ultimately to the relevant output functionals of the simulation. Standard sampling techniques, such as Monte Carlo, are "exact" methods for accounting for this type of uncertainty quantification in the sense that they do not require any approximations of the CFD analysis nor any assumptions on the input PDFs. Moreover, sampling techniques provide the full set of output statistics, albeit with obvious limitations on accuracy related to the number of samples. However, standard Monte Carlo is clearly intractable for large CFD problems

*School of Computational Science and Information Technology, Florida State University, Tallahassee, FL 32306-4120

†School of Computational Science and Information Technology, Florida State University, Tallahassee, FL 32306-4120

‡Associate Fellow, AIAA, NASA Langley Research Center, Hampton, VA 23681-2199

§CETHIL, UMR 5008, INSA, Villeurbanne 69621, France

as it easily requires thousands of simulations for meaningful results. Although more sophisticated sampling techniques such as importance sampling and Latin hypercube sampling are well-established, we are unaware of any attempts yet to use these for CFD applications. Cao, Hussaini and Zang[25] have recently presented a non-standard variance reduction technique that exploits sensitivity derivatives. They demonstrated that it reduces the sampling requirements by at least one order of magnitude on an aircraft wing structural application. This approach seems ideally suited to CFD applications with a large number of input uncertainty variables provided that the CFD code can produce efficient sensitivity derivatives.

The moment methods are an efficient approximate approach. They involve expanding the variables of the problem in terms of Taylor series around their mean value.[26] This technique allows for a quick estimation of the low-order statistics, but requires at a minimum an efficient procedure for computing first-order sensitivity derivatives.

In this paper we explore the use of a stochastic PDE approach, *i.e.*, adding one or more stochastic variables to the deterministic CFD equations, as an alternative to sampling techniques. Xiu and Karniadakis[27–29] pioneered the stochastic PDE approach to uncertainty quantification for CFD. They used a (generalized) Polynomial Chaos (PC) expansion method. This is based on the homogeneous chaos expansions introduced by Wiener[30] and extended and applied extensively by Ghanem and Spanos[31,32] for stochastic PDE solutions to structural problems. Walters and Huyse[22] include Polynomial Chaos examples in their tutorial. Walters[14] has explained how to deal correctly with the grid movement terms necessary to compute the effects of geometric uncertainties in Polynomial Chaos applications. Our contributions here are (1) the extension of the CFD Polynomial Chaos approach to include a two-equation turbulence model and (2) a discussion of an alternative stochastic PDE approach, called Stochastic Collocation (SC), that we have recently developed.[33,34] The demonstrations of these methods are given for a quasi-one-dimensional nozzle flow.

Stochastic PDE Fundamentals

The basic idea of the Polynomial Chaos approach is to project the random variables of the problem onto a stochastic space spanned by a set of complete orthogonal polynomials Ψ that are functions of a random variable $\xi(\theta)$ where θ is a random event. The terms of the polynomial are functions of $\xi(\theta)$ and are thus functionals. Many types of random variables can be used: for example, $\xi(\theta)$ can be a Gaussian variable associated with Hermite polynomials.

The original form of Polynomial Chaos was restricted to expansions in Hermite polynomials. Xiu and Karniadakis[28] generalized this concept to expansions in Askey polynomials, *e.g.*, Laguerre polynomials for random variables with a Gamma distribution, and Jacobi polynomials for Beta distributions. Obviously, the convergence rate, and thus the number of terms in the expansion required for a given accuracy, depends both on the random process to be approximated and on the choice of expansion functions.

We confine ourselves to Hermite expansions in the present work. Using this approach, each dependent variable of the problem is expanded as, say for the velocity u:

$$u(\boldsymbol{x},t,\theta) = \sum_{i=0}^{\infty} u_i(\boldsymbol{x},t)\ \Psi_i(\xi(\theta))\ . \tag{1}$$

For practical simulations, the series has to be truncated to a finite number of terms, hereafter denoted N_{PC}. This framework remains valid also for multiple random variables, including uncorrelated or partially correlated random variables. In that case, the dependent variables of the problem are functions of several independent random variables and $\boldsymbol{\xi}$ is now a vector. The expression for the multidimensional Hermite polynomial or order n, H_n, is

$$H_n(\xi_{i_1},\ldots,\xi_{i_n}) = (-1)^n e^{\frac{1}{2}\,\boldsymbol{\xi}^T\,\boldsymbol{\xi}} \frac{\partial^n}{\partial\xi_{i_1}\ \ldots\ \partial\xi_{i_n}} e^{-\frac{1}{2}\,\boldsymbol{\xi}^T\,\boldsymbol{\xi}}. \tag{2}$$

The general expression for the Polynomial Chaos is given by

$$u(\boldsymbol{x},t,\theta) = \sum_{i=0}^{N_{PC}} u_i(\boldsymbol{x},t)\ \Psi_i(\boldsymbol{\xi}(\theta))\ , \tag{3}$$

with the number of terms N_{PC} determined from

$$N_{PC}+1\ =\ \frac{(n_{pc}+p_{pc})!}{n_{pc}!\,p_{pc}!}\ , \tag{4}$$

where p_{pc} is the order of the expansion and n_{pc} the dimensionality of the chaos, *i.e.*, the number of random variables. (Note that the dimensionality of the chaos is not the same as the number of physical dimensions of the problem.) It follows that N_{PC} grows very quickly with the dimension of the chaos and the order of the expansion.

In the case of the Hermite polynomials, the zero*th*-order term represents the mean value and the first-order term the Gaussian part, while higher orders

account for non-Gaussian contributions. The inner product in the stochastic space is expressed as

$$\langle f_1(\boldsymbol{\xi})\ f_2(\boldsymbol{\xi})\rangle \ = \ \int_{-\infty}^{\infty} f_1(\boldsymbol{\xi})\ f_2(\boldsymbol{\xi})\ w(\boldsymbol{\xi})\ d\boldsymbol{\xi}\ , \qquad (5)$$

where the weight function $w(\boldsymbol{\xi})$ is the n_{pc}-dimensional normal distribution

$$w(\boldsymbol{\xi}) = \frac{1}{\sqrt{(2\,\pi)^{n_{pc}}}}\ e^{-\frac{1}{2}\,\boldsymbol{\xi}^T\,\boldsymbol{\xi}}\ . \qquad (6)$$

In the L_2-norm, we thus get

$$\langle \Psi_i\ \Psi_j\rangle \ = \ \langle \Psi_i^2\rangle\ \delta_{ij}\ , \qquad (7)$$

where δ is the Kronecker operator. The statistics of any order for a variable or set of variables can be determined from their Polynomial Chaos expansions.[28]

In the Stochastic Collocation method for one random variable, the finite expression corresponding to (3) is

$$u(\boldsymbol{x},t,\alpha) = \sum_{i=0}^{N_q} u_i(\boldsymbol{x},t)\ h_i(\alpha)\ , \qquad (8)$$

where α is an artificial variable introduced to facilitate the collocation process (see below), h_i is the Lagrange interpolating polynomial corresponding to the collocation points in α-space, and N_q denotes the degree of the polynomial. Our development of the Stochastic Collocation method is driven both by our desire to obtain an accurate but less expensive alternative to Polynomial Chaos for computing uncertainty propagation and to widen its field of applicability to any form of nonlinear models.

In Section 3 we furnish the governing equations and uncertainty description for quasi-1D nozzle. The subsequent section covers the discretization procedures. Section 5 presents representative results for quasi-1D nozzle flow using Polynomial Chaos, and compares its computational cost with that of the Stochastic Collocation method.

Stochastic Quasi-One-Dimensional Nozzle Flow

As a first step in evaluating the stochastic PDE approach to uncertainty quantification for compressible, turbulent flow, the Polynomial Chaos and Stochastic Collocation techniques were applied to a quasi 1-D nozzle flow. The physics of the phenomena involved in a nozzle flow are well understood, and the configuration is simple enough to allow focusing on the stochastic treatment rather than on numerical problems, making this configuration an appropriate choice. Mathelin and Hussaini[35] presented initial results for inviscid quasi 1-D nozzle flow using Polynomial Chaos, and Mathelin, Hussaini and Zang[34] presented a more extensive discussion of the inviscid flow application, including some Stochastic Collocation results. Here we add both viscosity and a 2-equation turbulence model to explore the issues in extending this methodology to the full three-dimensional, compressible, Reynolds-averaged Navier-Stokes equations.

Laminar equations

The equations for laminar, viscous, quasi 1-D nozzle flow in conservative form are

$$\boldsymbol{Q}_t + \boldsymbol{F}_x = \boldsymbol{S}\ , \qquad (9)$$

where

$$\begin{aligned}
\boldsymbol{Q} &= \begin{pmatrix} \rho\,A \\ \rho\,u\,A \\ \rho\,E\,A \end{pmatrix} \\
\boldsymbol{F} &= \begin{pmatrix} \rho\,u\,A \\ \dfrac{3-\gamma}{2}\,\rho\,u^2\,A + (\gamma-1)\,\rho\,E\,A \\ -(\frac{4}{3}\,\mu)\,A\,\partial_x u \\ \gamma\,\rho\,u\,E\,A - \dfrac{\gamma-1}{2}\,\rho\,u^3\,A \\ -\frac{(\gamma-1)\,\overline{M}}{R}\ (\lambda)\ A\,\partial_x\left(E - \frac{u^2}{2}\right) \end{pmatrix} \\
\boldsymbol{S} &= \begin{pmatrix} 0 \\ (\gamma-1)\ \left[\rho\,E - \frac{\rho\,u^2}{2}\right]\ \partial A/\partial x \\ 0 \end{pmatrix} \qquad (10)
\end{aligned}$$

with ρ the density, u the velocity, A the nozzle cross-section area, and E the total energy; γ is the specific heat ratio ($\gamma = 1.4$ for diatomic gas), μ the laminar dynamic viscosity, λ the laminar thermal diffusivity, R the ideal gas constant, and $\overline{M}$ the fluid molar mass. The static pressure P has been removed from the above equations by making use of

$$E = \frac{P}{(\gamma-1)\,\rho}\ + \frac{1}{2}\,u^2\ . \qquad (11)$$

Turbulence equations

The turbulence model considered here is the standard 2-equation $k-\epsilon$ model. The reasons for that choice are that considering the geometry and the quasi 1-D assumption, there is no need for a sophisticated turbulence model. Meanwhile, the $k-\epsilon$ model has features which also allow us to study the impact of uncertainty in the model coefficients (C_μ, C_{ϵ_1} and C_{ϵ_2}) upon the simulated field behavior and characteristics.

The second and third components of $\boldsymbol{F}$ in (10) are modified by replacing the $(\frac{4}{3}\,\mu)$ term by

$$(\frac{4}{3}\,\mu + 2\,\rho\,\nu_t) \tag{12}$$

and the term (λ) by

$$(\lambda + \rho\,\frac{\nu_t}{Pr_t})\,. \tag{13}$$

respectively, where ν_t is the turbulent kinematic viscosity, and the turbulent Prandtl number $Pr_t = \frac{\mu_t}{\lambda_t}$ is assumed constant.

To these must be added the $k-\epsilon$ model equations, which reduce to

$$\frac{\partial}{\partial x}\,(\rho\,u\,k\,A) = \frac{\partial}{\partial x}\left[\rho\,A\,\left(\nu + \frac{\nu_t}{\sigma_k}\right)\,\frac{\partial k}{\partial x}\right] + 2\,\rho\,\nu_t\,A\,\left(\frac{\partial u}{\partial x}\right)^2 - \rho\,\epsilon\,A \tag{14}$$

and

$$\frac{\partial}{\partial x}\,(\rho\,u\,\epsilon\,A) = \frac{\partial}{\partial x}\left[\rho\,A\,\left(\nu + \frac{\nu_t}{\sigma_\epsilon}\right)\,\frac{\partial \epsilon}{\partial x_j}\right] + 2\,C_{\epsilon_1}\,\frac{\epsilon}{k}\,\rho\,\nu_t\,A\,\left(\frac{\partial u}{\partial x}\right)^2 - C_{\epsilon_2}\,\rho\,\frac{\epsilon^2}{k}\,A \tag{15}$$

for the steady state. Here, k is the turbulent kinetic energy, and ϵ is the turbulent dissipation rate. The turbulent viscosity coefficient is defined by

$$\nu_t = C_\mu\,\frac{k^2}{\epsilon}\,. \tag{16}$$

The standard values of the turbulence model coefficients are $C_{\epsilon_1} = 1.44, C_{\epsilon_2} = 1.92, C_\mu = 0.09, \sigma_k = 1.0$ and $\sigma_\epsilon = 1.3$.

Nozzle geometry uncertainty description

One source of uncertainty is in the nozzle shape, due to unavoidable manufacturing variability. Let $A(x)$ be Gaussian and partially correlated along the x direction following the covariance:

$$C_{AA}(x_1, x_2) = \sigma^2\,e^{-\frac{|x_1 - x_2|}{b}}\,, \tag{17}$$

where b is the correlation length and σ^2 the associated variance. The Karhunen-Loeve decomposition is used to represent the stochastic process in the standard manner. See Ref. 34 for more details on the Karhunen-Loeve expansion for this particular problem.

Test problem

The problem studied here is that of a supersonic diverging nozzle, as illustrated in Figure 1. The inflow conditions are a Mach number of 1.2, a 1-atmosphere static pressure and unit density. The nozzle starts at x = 0.3 m and ends at x = 5.5 m. Uncertainty is considered to arise from nozzle geometry, inlet boundary conditions (pressure, velocity and density) and turbulence model coefficients. Here, we consider $b = 20$ and $\sigma = 0.05$ as describing the nozzle variability in Eq. (17). Due to the rapid decay of the eigenvalues of the Karhunen-Loeve expansion, only the first two eigenfunctions are retained in the expansion which describes the nozzle geometry uncertainty. The resulting "fuzzy" cross-section area is plotted in Figure 2.

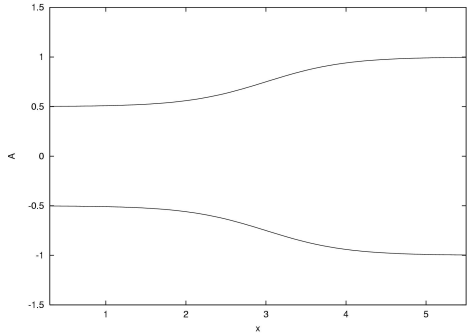

Fig. 1 Nozzle cross-section mean value along the streamwise distance.

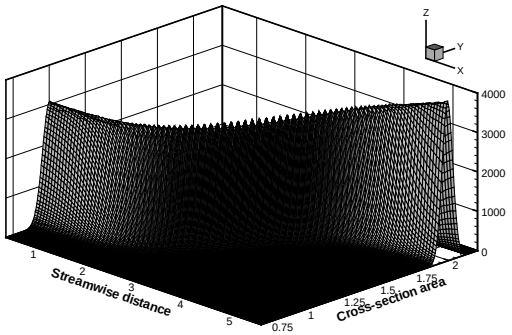

Fig. 2 Stochastic cross-section area Probability Density Function (PDF).

For turbulent flow, the additional inflow conditions are $k = 253$ m^2.s^{-2} (5 % turbulence intensity) and $\epsilon = 11,500$ m^2.s^{-3}. The mean value (from the turbulence point of view) results for turbulent flow are indistinguishable graphically from those for the inviscid flow.

Discretization

Physical space

The quasi 1-D equations are discretized using the spectral element method combined with a fourth order Runge–Kutta scheme in time. This spatial discretization is consistent with the spectral expansion involved in the Polynomial Chaos technique.

For simplicity, we will discuss only the inviscid problem in detail. The laminar version of Equation (10) is projected onto a spectral and stochastic basis and the Galerkin technique is applied. The spectral space is spanned by Chebyshev polynomials on the nodal points (in local coordinates $\overline{x} \in [-1;1]$):

$$\overline{x}_n = \cos\left(\frac{\pi\, n}{N}\right) \qquad \forall n \in [0;N] \subset \mathbb{N}\,, \tag{18}$$

where N is the number of points within each element.

The interpolants of variables, say u, in spectral space read as

$$u(\overline{x},t) = \sum_{n=0}^{N} u_n(t)\; h_n(\overline{x})\,, \tag{19}$$

where

$$h_n(\overline{x}) = \frac{2}{N}\; \sum_{m=0}^{N} \frac{1}{\overline{c}_n\; \overline{c}_m}\; T_m(\overline{x}_n)\; T_m(\overline{x})\,, \tag{20}$$

with T_m the Chebyshev polynomials and $\overline{c}_i$ such as

$$\overline{c}_i = 2 \qquad i \in \{0;N\} \;\subset \mathbb{N} \tag{21}$$

$$\overline{c}_i = 1 \qquad i \in \,]0;N[\quad \subset \mathbb{N}\,. \tag{22}$$

Polynomial Chaos

Similarly, in the stochastic space,

$$u(x,t,\theta) = \sum_{i=0}^{N_{PC}} u_i(x,t)\; \Psi_i(\xi(\theta))\,. \tag{23}$$

The following equation for the flux component of the momentum equation illustrates the computational complexity of the discretization for just the inviscid problem

$$\begin{aligned}
\frac{\partial F_2}{\partial x} \;=\; & \sum_{i=0}^{N_{PC}} \sum_{j=0}^{N_{PC}} \sum_{k=0}^{N_{PC}} \sum_{r=0}^{N_{PC}} \sum_{n=0}^{N} \sum_{m=0}^{N} \sum_{o=0}^{N} \\
& \frac{3-\gamma}{2}\; \rho_{i,n}\; u_{j,m}\; u_{k,o}\; \langle \Psi_i\; \Psi_j\; \Psi_k\; \Psi_r\; \Psi_l \rangle \\
& \left[(h_n, h_m, h_o, h_p)\; \frac{\partial A_k}{\partial x} A_k \left(\left(\frac{\partial h_n}{\partial x}, h_m, h_o, h_p \right) \right.\right. \\
& \left.\left. + \left(h_n, \frac{\partial h_m}{\partial x}, h_o, h_p \right) + \left(h_n, h_m, \frac{\partial h_o}{\partial x}, h_p \right) \right) \right] \\
& + (\gamma - 1) \sum_{i=0}^{N_{PC}} \sum_{j=0}^{N_{PC}} \sum_{k=0}^{N_{PC}} \sum_{n=0}^{N} \sum_{m=0}^{N} \rho_{i,n}\; E_{j,m} \\
& \langle \Psi_i\; \Psi_j\; \Psi_k\; \Psi_l \rangle \left[(h_n, h_m, h_p)\; \frac{\partial A_k}{\partial x} \right. \\
& \left. + A_k \left(\left(\frac{\partial h_n}{\partial x}, h_m, h_p \right) + \left(h_n, \frac{\partial h_m}{\partial x}, h_p \right) \right) \right]
\end{aligned} \tag{24}$$

The scalar products in the spectral space are defined by, say, for (h_n, h_m, h_o):

$$\begin{aligned}
(h_n, h_m, h_o) &= \int_{-1}^{1} h_n(\overline{x})\; h_m(\overline{x})\; h_o(\overline{x})\; d\overline{x} \\
&= \frac{8}{N^3} \sum_{a=0}^{N} \sum_{b=0}^{N} \sum_{c=0}^{N} \frac{T_a(\overline{x}_n)\; T_b(\overline{x}_m)\; T_c(\overline{x}_o)}{\overline{c}_a\; \overline{c}_b\; \overline{c}_c\; \overline{c}_n\; \overline{c}_m\; \overline{c}_o} \\
&\qquad \int_{-1}^{1} T_a(\overline{x})\; T_b(\overline{x})\; T_c(\overline{x})\; d\overline{x}\,.
\end{aligned} \tag{25}$$

In the stochastic space, we have for a 2-D Polynomial Chaos, *e.g.* $\langle \Psi_i\; \Psi_j\; \Psi_k\; \Psi_l \rangle$:

$$\begin{aligned}
& \langle \Psi_i\; \Psi_j\; \Psi_k\; \Psi_l \rangle = \\
& \frac{1}{\sqrt{(2\,\pi)^2}} \int_{-\infty}^{\infty} \int_{-\infty}^{\infty} \Psi_i\; \Psi_j\; \Psi_k\; \Psi_l\; e^{-\frac{1}{2}\, \boldsymbol{\xi}^T\, \boldsymbol{\xi}}\; d\boldsymbol{\xi}\,.
\end{aligned} \tag{26}$$

The full equations for the inviscid problem are available in Ref. 34. The nonlinearity in the inviscid momentum flux results in a 7-dimensional summation in Eq. (24). Four of these sums are due to the Polynomial Chaos expansion, and would remain even for a simple finite-difference spatial discretization.

The equations for the turbulence quantities ν_t, k and ϵ are given in the appendix in (31, 32, 33). The equation (33) for the turbulent kinetic energy, ϵ, contains a 12-dimensional sum, with seven of these due to the Polynomial Chaos terms. The stochastic collocation method presented in the following subsection was, in part, developed to reduce the cost of these multi-dimensional summations.

Stochastic Collocation

Let a and b be two independent random variables. In the Polynomial Chaos method, the finite series for

each variable would be expressed as, say, for a:

$$a = \sum_{i=0}^{N_{PC}} a_i \Psi_i(\xi) \ , \tag{27}$$

and the product ab would be

$$ab = \sum_{i=0}^{N_{PC}} \sum_{j=0}^{N_{PC}} a_i b_j \Psi_i(\xi) \Psi_j(\xi) \ . \tag{28}$$

(Here we drop any dependence upon x and t and concentrate on just the random variable ξ without reference to the random event parameter θ.)

The usual Galerkin truncation yields for the expansion coefficients of the product $c = ab$:

$$(ab)_k = \sum_{i=0}^{N_{PC}} \sum_{j=0}^{N_{PC}} a_i b_j \langle \Psi_i \Psi_j \Psi_k \rangle \quad \forall k \in [0; N_{PC}] \subset \mathbb{N}. \tag{29}$$

Therefore, computing the $N_{PC}+1$ coefficients of the product ab theoretically takes of order N_{PC}^3 operations and the complexity becomes even greater for cubic products. Moreover, this method cannot easily handle highly nonlinear equations, *e.g.* involving geometric functions. In particular, this is of critical importance in case the equations are solved using the popular discontinuous Galerkin spectral element method. This method requires a Riemann problem to be solved at each interface between two adjacent elements. Solving the Riemann problem involves non-linear equations, comprising geometric and discontinuous functions (see Sod,[36] for example). The stochastic collocation scheme is thus needed.

The usual spatial collocation consists in projecting the equations into the physical space ($\overline{x}$). But the stochastic space and its random variable counterpart θ have limited physical meaning and the spatial scheme cannot be directly transformed. To deal with this barrier, Mathelin and Hussaini[33] developed a "stochastic collocation" method. For the example given above, the method consists of the following. Starting from the PDF of a, construct the cumulative distribution function (CDF) of a. Use the (monotonic, one-to-one) CDF (after linearly mapping its range from [0,1] to [-1,1]) as a mapping to transform the random variable ξ from its space $]-\infty, +\infty[$ for the distributions used in this work) into the artificial variable $\alpha \in [-1, 1]$. Compute the N_qth-order Legendre polynomial expansion of the stochastic part of a in the new variables α, using the standard Gauss-Legendre quadrature points. Perform a similar process on b. Then use Gauss-Legendre numerical integration to compute the counterpart of (29) in α-space. This produces the stochastic collocation approximation to the CDF (albeit mapped to $[-1, 1]$) of the product (28). Finally, map this function back to $[0, 1]$, and differentiate it to obtain the desired PDF of the nonlinear term. The cost of this process is linear in N_q, regardless of the nature of the nonlinear term.

Mathelin and Hussaini[33] demonstrated that this method successfully solved a stochastic Riemann problem in which the initial state contained a discontinuity, but the variables had prescribed PDFs rather than being deterministic. There are numerous open issues with the stochastic collocation approach, especially on how best to perform the transformations. At present, a brute-force approach with $N_q = 200$ has been used to demonstrate that the method works.

Sample Results

Polynomial Chaos validation

The Polynomial Chaos (PC) approach was first compared to Monte Carlo simulations for the inviscid problem. The method used here is the regular MC method and does not take advantage of any accelerating technique. All the inlet conditions are set Gaussian and fully correlated. The cross-section area is here assumed deterministic. Monte Carlo simulations are carried with over 9 million independent samples while the Polynomial Chaos is 1-D, second order, *i.e.*, there is one independent random variable and second-order Hermite polynomial expansions are used.

Figure 3 shows the comparison between the Probability Density Function (PDF) obtained from the Monte Carlo and Polynomial Chaos techniques for the density and velocity at the outlet of the nozzle. The density (and pressure) PDFs remain approximately Gaussian at the nozzle exit while the velocity PDF becomes skewed due to non-linearity in the Euler equations. It can be seen that an excellent agreement between the two techniques is achieved, especially for the density where the two curves almost match. For the velocity, the agreement is very good except in the left tail region, indicating the need for higher order in the PC expansion to improve the approximation. Meanwhile, this example clearly demonstrates the ability of the PC technique to accurately propagate uncertainty throughout the flow, even with a very limited number of terms in the expansion (3 terms in this case). Considering the difference in the CPU time required (1.7×10^6 s for MC, 70 s for PC), the speed-up ratio is approximately 24,000, hence making the PC a much more effective alternative to the Monte Carlo technique for this case. The cost of a single inviscid computation

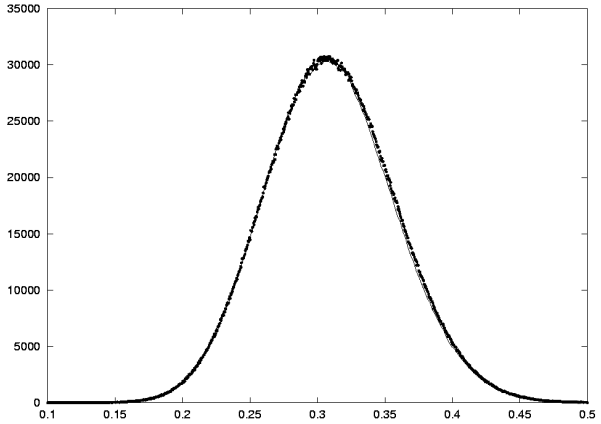

a) Density.

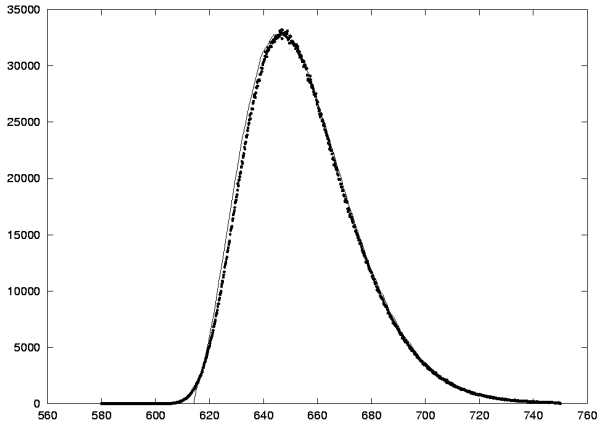

b) Velocity.

Fig. 3 Outlet probability density function. 1-D $2nd$ order Polynomial Chaos (solid line) vs Monte Carlo (dots). Arbitrary units.

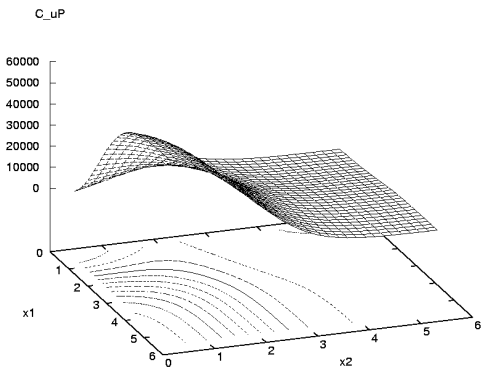

a) Velocity / Pressure.

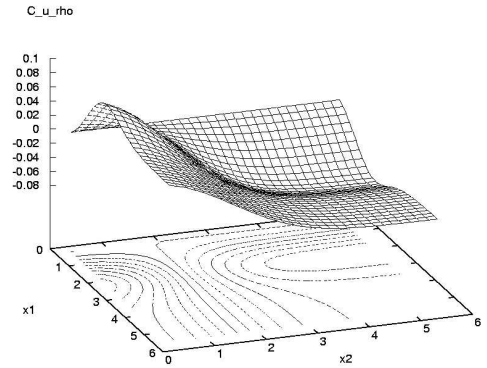

b) Velocity / Density.

Fig. 4 Distribution of the covariance.

using 1-D, second-order PC takes roughly 13 times longer than a single inviscid, deterministic solution.

2-D stochastic simulations

When the random variables of the problem considered are decoupled or, at most, only partially correlated, the stochastic process must be described using several independent random variables ξ. To illustrate this more general problem, a 2-D, $2nd$-order PC inviscid simulation is reported in this section. The inlet pressure and velocity are both assumed uncertain with no correlation while the inlet density is considered to be deterministic. Inlet pressure uncertainty is spanned along the stochastic dimension ξ_1 while velocity uncertainty is spanned along dimension ξ_2. The nozzle shape, A, is assumed uncertain as well and is expanded in a 2-D Karhunen-Loeve series. All variables are now expanded in 6 terms within the stochastic space.

In Figure 4, the covariance distribution is plotted for $u - P$ and $u - \rho$. Since all variables are set independent at the inlet, the covariance is zero at that point for all combinations. Downstream, coupling effects spread the uncertainty across the different variables, and the covariance evolves towards a steady state near the outlet of the nozzle.

Turbulence simulation

Four separate viscous, turbulent cases have been run. In each case the PC is 1-D, second order. In each case the relevant variable is assumed Gaussian: (a) the inlet velocity u_{inlet} has a mean value of 450 m.s^{-1} with a 10 m.s^{-1} standard deviation; (b) the coefficient C_μ has a mean of 0.09 with a 10% standard deviation (=0.009); (c) the coefficient C_{ϵ_1} has a mean of 1.44 with a 0.1 standard deviation; and (d) the coefficient C_{ϵ_2} has a mean of 1.92 with a 0.1 standard deviation.

The effects of these uncertainties upon the mean values of ρ, u and P are negligible. A more noticeable effect is upon the deviation of the turbulent flow variables k and ϵ from their deterministic values. These are illustrated in Figure 5. The inlet velocity uncertainty affects the turbulent kinetic energy and the turbulent dissipation rate to about the same extent. The uncertainty in the modeling parameter C_{ϵ_1} has its greatest effect upon the turbulent dissipation rate, whereas the paramter C_μ has a strong effect upon the turbulent kinetic energy. The uncertainty in the modeling parameter C_{ϵ_2} has a much smaller effect than the uncertainties in the other three quantities.

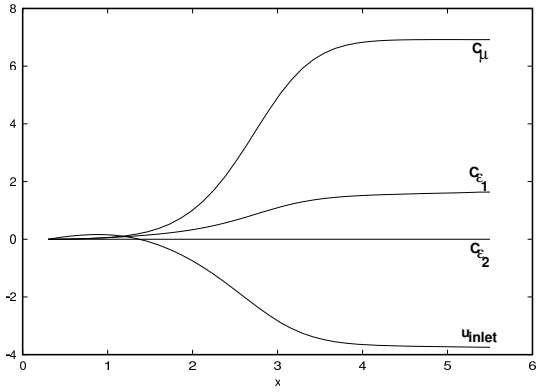

a) Turbulent Kinetic Energy.

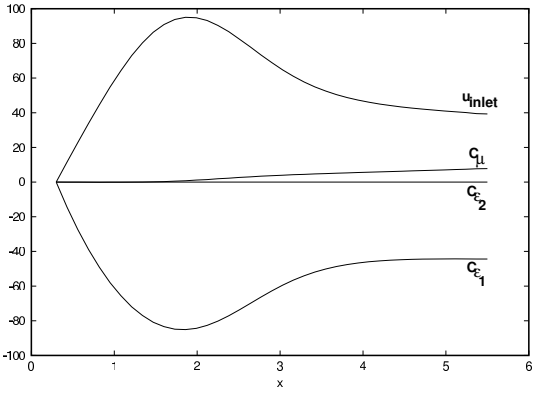

b) Turbulent Dissipation Rate.

Fig. 5 Distribution of the deviation of the turbulence quantities.

Relative cost of Polynomial Chaos and Stochastic Collocation

The most complex nonlinearity arises for the third component of the inviscid momentum flux (24), which requires a 9-dimensional summation. Five of these sums are due to the Polynomial Chaos expansion, and would remain even for a simple finite-difference spatial discretization. Thus, the cost of the stochastic part of the Polynomial Chaos method for the quasi-1D nozzle problem scales as $(N_{PC}+1)^5$. In contrast, the cost of the Stochastic Collocation method scales linearly with N_q. For the turbulent case, the stochastic part of the Polynomial Chaos method scales as $(N_{PC}+1)^7$, whereas, the cost of the Stochastic Collocation Method still scales linearly with N_q. The precise coefficients in front of these scaling terms are very problem dependent. We illustrate the relative cost of the two methods for computations with a single stochastic variable using either $N_{PC}+1 = 4$ for third-order Polynomial Chaos (see (4)) or $N_q = 200$ for Stochastic Collocation. In the first row of Table 1, we present CPU timings (in seconds on a PC) for the two methods on the inviscid quasi-1D nozzle problem with $N = 31$ points in physical space (15 elements and 3 points per element). Clearly, the Stochastic Collocation method provides a significant reduction in cost. The second row gives the timing of the Polynomial Chaos method on the turbulent problem. Results for the Stochastic Collocation method are not yet available for the turbulent problem, but we anticipate that the cost of the Stochastic Collocation computations for a turbulent case will be a full order of magnitude lower than for Polynomial Chaos. The gap between SC and PC methods will be even larger when comparing simulations with two independent random variables.

	Deter.	PC_{1D}	SC_{1D}	PC_{2D}
inviscid	19	1,760	298	93,600
turbulent	22	3,484	N/A	185,286

Table 1 CPU time requirements (seconds on a PC)

Concluding Remarks

The major barrier to the application of traditional sampling methods to uncertainty quantification in CFD is the explosion in computational cost. Stochastic methods such as Polynomial Chaos and Stochastic Collocation hold the promise of making uncertainty quantification feasible, at least for a small number of random variables. The Stochastic Collocation method appears to have distinct advantages over the more established (but still relatively novel) Polynomial Chaos approach. However, considerable work is needed to make the Stochastic Collocation both more efficient and more rigorous.

Acknowledgement

The work of the first and second authors was supported by NASA Cooperative Agreement NCC-1-02025.

References

[1]U. B. Mehta, *Some aspects of uncertainty in computational fluid dynamics results*, J. Fluids Eng., Vol. 113, pp. 538–543, 1991.

[2]P. J. Roache, *Verification and validation in computational science and engineering*, Hermosa Publishers, Albuquerque, 1998.

[3]H. W. Coleman and F. Stern, *Uncertainties and CFD code validation*, J. Fluids Eng., Vol. 119, pp. 795–803, 1997.

[4]W. L. Oberkampf and F. G. Blottner, *Issues in computational fluid dynamics code verification and validation*, AIAA J., Vol. 36, No. 5, pp. 687–695, 1998.

[5]Anon., *AIAA guide for the verification and validation of computational fluid dynamics simulations*, AIAA G-077-1998, 1998.

[6]M. J. Hemsch, *Statistical analysis of CFD solutions from the drag prediction workshop*, AIAA 2002–0842, 2002. (See also http://ad-www.larc.nasa.gov/tsab/cfdlarc/aiaa-dpw/ for links to all the presentations at the workshop.)

[7]R. R. Cosner, *The importance of uncertainty estimation in Computational Fluid Dynamics*, AIAA-2003-0406, 2003.

[8]E. N. Tinoco and J. E. Bussoletti, *Minimizing CFD uncertainty for commercial aircraft applications*, AIAA-2003-0407, 2003.

[9]P. J. Roache, *Error bars for CFD*, AIAA-2003-0408, 2003.

[10]J. M. Luckring, M. J. Hemsch and J. H. Morrison, *Uncertainty in computational aerodynamics*, AIAA 2003–0409, 2003.

[11]F. Stern, R. Wilson and J. Shao, *Statistical approach to CFD code certification*, AIAA-2003-0410, 2003.

[12]M. R. Mendenhall, R. E. Childs and J. H. Morrison, *Best practices for reduction of uncertainty in CFD results*, AIAA-2003-0411, 2003.

[13]D. Pelletier, *Uncertainty analysis by the sensitivity equation method*, AIAA-2003-0412, 2003.

[14]R. W. Walters, *Towards stochastic fluid mechanics via Polynomial Chaos*, AIAA 2003-0413, 2003.

[15]U. Ghia, *ASMEs quest to quantify numerical uncertainty*, AIAA-2003-0627, 2003.

[16]I. Celik, G. Hu and A. Badeau, *Further refinement and bench marking of a single-grid error estimation technique*, AIAA-2003-0628, 2003.

[17]C. J. Roy and M. M. Hopkins, *Discretization error estimates using exact solutions to nearby problems*, AIAA-2003-0629, 2003.

[18]K. M. Hanson and F. M. Hemez, *Uncertainty quantification of simulation codes based on experimental data*, AIAA-2003-0630, 2003.

[19]R. W. Logan and C. K. Nitta, *Validation, uncertainty, and quantitative reliability at confidence*, AIAA-2003-1337, 2003.

[20]W. L. Oberkampf, K. V. Diegert, K F. Alvin and B. M. Rutherford, *Variability, uncertainty, and error in computational simulation*, AIAA/ASME Joint Thermophysics and Heat Transfer Conference, ASME-HTD-Vol. 357-2, pp. 259272, 1998.

[21]W. L. Oberkampf and T. G. Trucano, *Verification and validation in computational fluid dynamics*, Progress Aerospace Sci., in press.

[22]R. W. Walters and L. Huyse, *Uncertainty analysis for fluid mechanics with applications*, ICASE Report No. 2002-1, 2002*.

[23]T. A. Zang, M. J. Hemsch, M. W. Hilburger, S. P. Kenny, J. M. Luckring, P. Maghami, S. L. Padula and W. J. Stroud *Needs and opportunities for uncertainty-based multidisciplinary design methods for aerospace vehicles*, NASA/TM-2002-211462, July 2002*.

[24]W. L. Oberkampf, J. C. Helton and K.Sentz, *Mathematical representation of uncertainty*, AIAA-2001-1645, 2001.

[25]Y. Cao, M. Y. Hussaini and T. A. Zang, *On the exploitation of sensitivity derivatives for improving sampling methods*, AIAA 2003-1656, 2003*.

[26]A. C. Taylor, L. L. Green, P. A. Newman and M. M. Putko, *Some advanced concepts in discrete aerodynamic sensitivity analysis*, AIAA 2001-2529, 2001*.

[27]D. Xiu, D. Lucor, C.-H. Su and G. Em. Karniadakis, *Stochastic modeling of flow-structure interactions using generalized polynomial chaos*, J. Fluids Eng., Vol. 124, No. 1, pp. 51–59, 2002.

[28]D. Xiu and G. Em. Karniadakis, *The Wiener-Askey polynomial chaos for stochastic differential equations*, SIAM J. Sci. Comput., Vol. 24, No. 2, pp. 619–644, 2002.

[29]D. Xiu D. and G. Em. Karniadakis, *Modeling uncertainty in flow simulations via generalized polynomial chaos*, J. Comput. Phys., Vol. 187, No. 1, pp. 137–167, 2003.

[30]N. Wiener, *The homogeneous chaos*, Amer. J. Math., Vol. 60, pp. 897–936, 1938.

[31]R. G. Ghanem and P. D. Spanos, *Stochastic finite elements: a spectral approach*, Springer-Verlag, New-York, 1991.

[32]R. Ghanem, *Ingredients for a general purpose stochastic finite elements implementation*, Comput. Methods Appl. Mech. Engrg., Vol. 168, pp. 19–34, 1999.

[33]L. Mathelin and M. Y. Hussaini, *A stochastic collocation algorithm for uncertainty analysis*, NASA/CR–2003–212153, February 2003*.

[34]L. Mathelin, M. Y. Hussaini and T. A. Zang, *Stochastic approaches to uncertainty quantification in CFD simulations*, Numerical Algorithms, submitted.

[35]L. Mathelin and M. Y. Hussaini, *Uncertainty quantification in CFD simulations: a stochastic spectral approach*, 2nd International Conference on Computational Fluid Dynamics, Sydney, Australia, July 15-19, 2002.

[36]G. A. Sod, *A survey of several finite difference methods for systems of nonlinear hyperbolic conservation laws*, J. Comput. Phys., Vol. 27, pp. 1–31, 1978.

*available online at http://ltrs.larc.nasa.gov

Appendix

The equations on the following page give the full Galerkin Polynomial Chaos expressions for ν_t, k, ϵ and a representative scalar product in the spectral space. In the stochastic space, we have for a 2-D Polynomial Chaos, *e.g.*,

$$< \Psi_a \, \Psi_b \, \Psi_c \, \Psi_d \, \Psi_e > = \frac{1}{\sqrt{(2\,\pi)^2}} \int_{-\infty}^{\infty} \int_{-\infty}^{\infty} \Psi_a \, \Psi_b \, \Psi_c \, \Psi_d \, \Psi_e \, e^{-\frac{1}{2}\,\boldsymbol{\xi}^T\,\boldsymbol{\xi}} \, d\boldsymbol{\xi} \, . \tag{30}$$

$\boldsymbol{\nu_t}$:

$$\begin{aligned}
&\sum_{i=0}^{N}\sum_{j=0}^{N}\sum_{a=0}^{Npc}\sum_{b=0}^{Npc}\nu_{i,a}\,\epsilon_{j,b}\;<\Psi_a\,\Psi_b\,\Psi_p>\;(h_i,h_j,h_k)\\
&=\sum_{i=0}^{N}\sum_{j=0}^{N}\sum_{a=0}^{Npc}\sum_{b=0}^{Npc}\sum_{c=0}^{Npc}C_{\mu_c}\,k_{i,a}\,k_{j,b}\;<\Psi_a\,\Psi_b\,\Psi_c\,\Psi_p>\;(h_i,h_j,h_k)
\end{aligned}\tag{31}$$

$\boldsymbol{k}$:

$$\begin{aligned}
&\sum_{i=0}^{N}\sum_{j=0}^{N}\sum_{l=0}^{N}\sum_{a=0}^{Npc}\sum_{b=0}^{Npc}\sum_{c=0}^{Npc}\sum_{d=0}^{Npc}\rho_{i,a}\,U_{j,b}\,k_{l,c}\;<\Psi_a\,\Psi_b\,\Psi_c\,\Psi_d\,\Psi_p>\\
&\left\{A_d\left[\left(\frac{\partial h_i}{\partial\overline{x}},h_j,h_l,h_k\right)+\left(h_i,\frac{\partial h_j}{\partial\overline{x}},h_l,h_k\right)+\left(h_i,h_j,\frac{\partial h_l}{\partial\overline{x}},h_k\right)\right]+\frac{\partial A_d}{\partial x}\;(h_i,h_j,h_l,h_k)\right\}\\
&-(-1)\sum_{i=0}^{N}\sum_{j=0}^{N}\sum_{l=0}^{N}\sum_{a=0}^{Npc}\sum_{b=0}^{Npc}\sum_{c=0}^{Npc}\sum_{d=0}^{Npc}\rho_{i,a}\,\nu_{j,b}\,k_{l,c}\,A_d\;<\Psi_a\,\Psi_b\,\Psi_c\,\Psi_d\,\Psi_p>\;\left(h_i,h_j,\frac{\partial h_l}{\partial\overline{x}},\frac{\partial h_k}{\partial\overline{x}}\right)\\
&\quad=2\sum_{i=0}^{N}\sum_{j=0}^{N}\sum_{l=0}^{N}\sum_{m=0}^{N}\sum_{a=0}^{Npc}\sum_{b=0}^{Npc}\sum_{c=0}^{Npc}\sum_{d=0}^{Npc}\sum_{e=0}^{Npc}\rho_{i,a}\,\nu_{j,b}\,U_{l,c}\,U_{m,d}\,A_e\\
&<\Psi_a\,\Psi_b\,\Psi_c\,\Psi_d\,\Psi_e\,\Psi_p>\;\left(h_i,h_j,\frac{\partial h_l}{\partial\overline{x}},\frac{\partial h_m}{\partial\overline{x}},h_k\right)\\
&\quad-\sum_{i=0}^{N}\sum_{j=0}^{N}\sum_{a=0}^{Npc}\sum_{b=0}^{Npc}\sum_{c=0}^{Npc}\rho_{i,a}\,\epsilon_{j,b}\,A_c\;<\Psi_a\,\Psi_b\,\Psi_c\,\Psi_p>\;(h_i,h_j,h_k)
\end{aligned}\tag{32}$$

$\boldsymbol{\epsilon}$:

$$\begin{aligned}
&\sum_{i=0}^{N}\sum_{j=0}^{N}\sum_{l=0}^{N}\sum_{m=0}^{N}\sum_{a=0}^{Npc}\sum_{b=0}^{Npc}\sum_{c=0}^{Npc}\sum_{d=0}^{Npc}\sum_{d=0}^{Npc}\rho_{i,a}\,U_{j,b}\,k_{l,c}\,\epsilon_{m,d}\;<\Psi_a\,\Psi_b\,\Psi_c\,\Psi_d\,\Psi_e\,\Psi_p>\\
&\left\{A_e\left[\left(\frac{\partial h_i}{\partial\overline{x}},h_j,h_l,h_m,h_k\right)+\left(h_i,\frac{\partial h_j}{\partial\overline{x}},h_l,h_m,h_k\right)+\left(h_i,h_j,h_l,\frac{\partial h_m}{\partial\overline{x}},h_k\right)\right]+\frac{\partial A_e}{\partial x}\;(h_i,h_j,h_l,h_m,h_k)\right\}\\
&-(-1)\sum_{i=0}^{N}\sum_{j=0}^{N}\sum_{l=0}^{N}\sum_{m=0}^{N}\sum_{a=0}^{Npc}\sum_{b=0}^{Npc}\sum_{c=0}^{Npc}\sum_{d=0}^{Npc}\sum_{e=0}^{Npc}\rho_{i,a}\,\nu_{j,b}\,k_{l,c}\,\epsilon_{m,d}\,A_e\\
&<\Psi_a\,\Psi_b\,\Psi_c\,\Psi_d\,\Psi_e\,\Psi_p>\;\left[\left(h_i,h_j,h_l,\frac{\partial h_m}{\partial\overline{x}},\frac{\partial h_k}{\partial\overline{x}}\right)+\left(h_i,h_j,\frac{\partial h_l}{\partial\overline{x}},\frac{\partial h_m}{\partial\overline{x}},h_k\right)\right]\\
&\quad=2\sum_{i=0}^{N}\sum_{j=0}^{N}\sum_{l=0}^{N}\sum_{m=0}^{N}\sum_{o=0}^{N}\sum_{a=0}^{Npc}\sum_{b=0}^{Npc}\sum_{c=0}^{Npc}\sum_{d=0}^{Npc}\sum_{e=0}^{Npc}\sum_{f=0}^{Npc}\sum_{g=0}^{Npc}C_{\epsilon_1 g}\,\rho_{i,a}\,\nu_{j,b}\,U_{l,c}\,U_{m,d}\,\epsilon_{o,e}\,A_f\\
&<\Psi_a\,\Psi_b\,\Psi_c\,\Psi_d\,\Psi_e\,\Psi_f\,\Psi_g\,\Psi_p>\left(h_i,h_j,\frac{\partial h_l}{\partial\overline{x}},\frac{\partial h_m}{\partial\overline{x}},h_o,h_k\right)\\
&-\sum_{i=0}^{N}\sum_{j=0}^{N}\sum_{L=0}^{N}\sum_{a=0}^{Npc}\sum_{b=0}^{Npc}\sum_{c=0}^{Npc}\sum_{d=0}^{Npc}\sum_{e=0}^{Npc}C_{\epsilon_2 e}\,\rho_{i,a}\,\epsilon_{j,b}\,\epsilon_{l,c}\,A_d\;<\Psi_a\,\Psi_b\,\Psi_c\,\Psi_d\,\Psi_e\,\Psi_p>\;(h_i,h_j,h_l,h_k)
\end{aligned}\tag{33}$$

typical inner product:

$$\begin{aligned}
\left(h_i,\frac{\partial h_j}{\partial\overline{x}},\frac{\partial h_l}{\partial\overline{x}},h_m,h_k\right) &= \int_{-1}^{1}h_i(\overline{x})\,\frac{\partial h_j}{\partial\overline{x}},\frac{\partial h_l}{\partial\overline{x}}\,h_m(\overline{x})\,h_k(\overline{x})\,d\overline{x}\\
&= \frac{32}{N^5}\sum_{a=0}^{N}\sum_{b=0}^{N}\sum_{c=0}^{N}\sum_{d=0}^{N}\sum_{e=0}^{N}\frac{T_a(\overline{x}_i)\,T_b(\overline{x}_j)\,T_c(\overline{x}_l)\,T_d(\overline{x}_m)\,T_e(\overline{x}_k)}{\overline{c}_a\,\overline{c}_b\,\overline{c}_c\,\overline{c}_d\,\overline{c}_e\,\overline{c}_i\,\overline{c}_j\,\overline{c}_l\,\overline{c}_m\,\overline{c}_k}\\
&\qquad\int_{-1}^{1}T_a(\overline{x})\,\frac{\partial T_b(\overline{x})}{\partial\overline{x}}\,\frac{\partial T_c(\overline{x})}{\partial\overline{x}}\,T_d(\overline{x})\,T_e(\overline{x})\,d\overline{x}
\end{aligned}\tag{34}$$